Neurosci. Bull. April, 2021, 37(4):478–496
https://doi.org/10.1007/s12264-020-00617-0

www.neurosci.cn
www.springer.com/12264

ORIGINAL ARTICLE

Tweety-Homolog 1 Facilitates Pain *via* Enhancement of Nociceptor Excitability and Spinal Synaptic Transmission

Wen-Juan Han[1,2] · Sui-Bin Ma[2] · Wen-Bin Wu[3] · Fu-Dong Wang[3] · Xiu-Li Cao[4] · Dong-Hao Wang[5] · Hai-Ning Wu[1] · Rou-Gang Xie[2] · Zhen-Zhen Li[2] · Fei Wang[2] · Sheng-Xi Wu[2] · Min-Hua Zheng[4] · Ceng Luo[2] · Hua Han[1]

Received: 15 March 2020 / Accepted: 9 June 2020 / Published online: 23 December 2020

Abstract Tweety-homolog 1 (Ttyh1) is expressed in neural tissue and has been implicated in the generation of several brain diseases. However, its functional significance in pain processing is not understood. By disrupting the gene encoding Ttyh1, we found a loss of Ttyh1 in nociceptors and their central terminals in Ttyh1-deficient mice, along with a reduction in nociceptor excitability and synaptic transmission at identified synapses between nociceptors and spinal neurons projecting to the periaqueductal grey (PAG) in the basal state. More importantly, the peripheral inflammation-evoked nociceptor hyperexcitability and spinal synaptic potentiation recorded in spinal-PAG projection neurons were compromised in Ttyh1-deficient mice. Analysis of the paired-pulse ratio and miniature excitatory postsynaptic currents indicated a role of presynaptic Ttyh1 from spinal nociceptor terminals in the regulation of neurotransmitter release. Interfering with Ttyh1 specifically in nociceptors produces a comparable pain relief. Thus, in this study we demonstrated that Ttyh1 is a critical determinant of acute nociception and pain sensitization caused by peripheral inflammation.

Keywords Ttyh1 · Inflammatory pain · Peripheral sensitization · Long-term potentiation

Wen-Juan Han, Sui-Bin Ma, and Wen-Bin Wu authors have contributed to this work equally.

✉ Min-Hua Zheng
zhengmh@fmmu.edu.cn

✉ Ceng Luo
luoceng@fmmu.edu.cn

✉ Hua Han
huahan@fmmu.edu.cn

[1] Department of Biochemistry and Molecular Biology, School of Basic Medicine, Fourth Military Medical University, Xi'an 710032, China

[2] Department of Neurobiology, School of Basic Medicine, Fourth Military Medical University, Xi'an 710032, China

[3] The Fourth Regiment, School of Basic Medicine, Fourth Military Medical University, Xi'an 710032, China

[4] Department of Medical Genetics and Developmental Biology, Fourth Military Medical University, Xi'an 710032, China

[5] National Engineering Laboratory for Resource Development of Endangered Crude Drugs in Northwest China, Key Laboratory of Medicinal Resources and Natural Pharmaceutical Chemistry, Ministry of Education, College of Life Sciences, Shaanxi Normal University, Xi'an 710119, China

Introduction

Chronic pain is an important public health problem that seriously affects the quality of life. Pain is a complex subjective phenomenon: it is a series of unpleasant feelings and emotional experiences after tissue or nerve injury [1, 2]. Patients with chronic pain often experience spontaneous ongoing pain, hyperalgesia (increased pain in response to noxious stimuli), and allodynia (pain evoked by non-noxious stimuli) [3–5]. Despite considerable progress in the understanding of chronic pain in the past few decades [2], treatment options have been mainly confined to opioids and nonsteroidal anti-inflammatory drugs [6–10]. Moreover, intervention with these therapeutics is associated with serious central side-effects, such as addiction, tolerance, and peptic ulcers, which in turn hamper medical adherence [7, 10]. Therefore, it is very important to improve the understanding of chronic pain mechanisms

and find new therapeutic targets for better therapeutics with minimal side-effects.

The *Drosophila melanogaster* tweety (*tty*) gene was originally found to be a transcription unit adjacent to the *flightless* gene [11]. Based on phylogenetic analysis, the tty family is highly conserved and has three homologues in mammals (Ttyh1, Ttyh2, and Ttyh3) [12–14]. According to sequence prediction, the Tweety family proteins contain five or six transmembrane domains, and are considered to be chloride (Cl^-) channels with large conductance, Ttyh1 acting as a volume-regulated Cl^- channel and the other two subunits (Ttyh2 and Ttyh3) acting as Ca^{2+}-activated Cl^- channels [14–16]. Given their mainly restricted localization to neural tissues [17], the association of Ttyh1 with fundamental cellular processes as well as several brain diseases has aroused great interest. For example, Ttyh1 is strongly upregulated in several pathological conditions such as epilepsy [18, 19] and childhood brain tumors [20]. Ectopic expression of Ttyh1 in human renal epithelial cells results in long, branched filopodia while its overexpression in cultured rat hippocampal neurons results in strong neurofibrillation and complex dendritic trees [17, 18]. Deficiency of Ttyh1 is closely related to disturbance of early embryonic development [21–23]. Of note, among neural tissues, Ttyh1 is predominantly expressed in the dorsal root ganglion (DRG) and spinal cord, where the first-order primary sensory neurons and the first synapse are located in the nociceptive pathway [22, 24]. There is a great deal of evidence that primary sensory neurons and their synaptic plasticity with spinal dorsal horn (SDH) neurons are the cellular basis of chronic pain [25–29]. However, it remains elusive whether Ttyh1 regulates pain and sensitization, and if so, what mechanisms underlie this regulation.

Here, we explored the role of Ttyh1 in DRG and spinal cord of pain circuit by combining an inflammatory pain model and behavioral investigation, biochemical analyses, and electrophysiological recordings as well as genetic manipulations. Our analyses revealed that Ttyh1 is densely expressed in the DRG and SDH, and is significantly upregulated following peripheral inflammation. Loss of Ttyh1 function ($Ttyh1^{-/-}$) leads to pain relief, in large part by decreasing the nociceptor hyperexcitability and spinal synaptic potentiation induced by inflammation. Interestingly, specific genetic ablation of Ttyh1 in nociceptors produces antinociception comparable to that in global $Ttyh1^{-/-}$ mice, designating Ttyh1 in nociceptors as a critical molecular determinant of pro-nociceptive transmission. Hence, targeting Ttyh1 in nociceptors may represent a novel therapeutic target for analgesia with minimal side-effects.

Materials and Methods

Animals

All animal procedures were reviewed and approved by the Institutional Animal Care and Use Committee of the Fourth Military Medical University. Mice were housed (up to five per cage) and maintained on a 12-h light/dark cycle with free access to food and water. All efforts were made to minimize the number of animals used in the study. Null mutant mice were obtained using the CRISPR-Cas9 technique as described previously [21]. $Ttyh1^{-/-}$ mice were crossed back into the C57Bl6 strain for more than eight generations. SNS-Cre mice were kindly provided by Prof. Rohini Kuner (University of Heidelberg, Germany). LoxP-flanked Ttyh1 shRNA-expressing AAV2/8 was provided by BrainVTA (Wuhan, China). In all experiments, littermates were used to strictly avoid genetic effects. All testing was conducted in a double-blinded manner. The experimenter was blind to treatment and/or genotype of mice throughout.

Behavioral Analysis

All the testing was carried out in accordance with the approved guidelines. All behavioral measurements were performed in conscious, unrestrained, and age-matched adult male mice. Before tests, the male mice were domesticated in the laboratory and habituated to the experimental setups.

Spontaneous pain observation: Before administration of the chemical agents, adult male mice were acclimated in a test chamber for at least 30 min. Then, $Ttyh1^{+/+}$ and $Ttyh1^{-/-}$ mice were injected with 20 μL capsaicin (0.06%; Sigma-Aldrich, USA) or formalin (1%; Sigma-Aldrich) into the intraplantar surface of the left hindpaw. Spontaneous pain responses were recorded continuously for 10 min in the capsaicin test and 60 min in the formalin test. The time that mice spent in flinching, lifting, and licking the injected hindpaw during 5-min intervals was recorded following formalin injection and during a 1-min interval for the capsaicin test [26, 30].

Mechanical nociception assay: Complete Freund's adjuvant (20 μL) (CFA, Sigma-Aldrich, USA) was unilaterally injected into the intraplantar surface of the hindpaw of adult male $Ttyh1^{+/+}$ and $Ttyh1^{-/-}$ mice. As described previously [26], the manual application of von Frey filaments ranging from 0.008 to 4.000 g to the plantar surface (Danmic Global, CA, USA) was used to measure basal mechanical sensitivity and at 6 h, 12 h, and 1, 2, 3, 7, and 14 days after CFA injection. The percentage of positive paw withdrawal responses to the stimulus was recorded 10 times for each filament applied. A positive response was a rapid paw withdrawal from the given stimulus filament. The 50% paw

withdrawal thresholds were determined and then averaged in the experimental groups.

Thermal nociception assay: Thermal sensitivity was assessed by applying infrared heating to the plantar surface of the hindpaw of adult male mice and the response latency was read from an automated device (IITC model 400, Woodland Hills, CA, USA), as described previously [26]. Each hindpaw was tested 5 times at 5-min intervals, and the withdrawal latency was averaged. To avoid tissue damage by prolonged thermal stimuli, the cutoff latency was set at 25 s.

Motor coordination testing: we used a Rotarod apparatus (XR1514, XinRuan, Shanghai, China) to test motor function, as described previously [59]. The velocity of rotation was increased from 0 to 60 rpm over a 180-s period. After adaptation and training, each adult male mouse was placed on the rotating rod and the falling latency was recorded.

Immunofluorescence Labelling

Deeply anesthetized with urethane (25%, 1.2 g/kg, i.p.) adult male mice were perfused transcardially. The L3/L4 DRGs and lumbar enlargement of the spinal cord were extracted, post-fixed, and cryoprotected. The tissues were cut on a cryostat at 20 μm for the DRG and 16 μm for the spinal cord. Immunofluorescence staining was performed using standard reagents and protocols. After incubation with bovine serum albumin (BSA, Kehao, Guangzhou, China), the sections were incubated with rabbit anti-calcitonin gene-related peptide (CGRP, 1:300; ab36001, Abcam), isolectin B4 (IB4, 1:300; DL-1207, Vector, Burlingame, CA, USA), rabbit anti-label for neurofilaments 200 (NF200, 1:300; N5389, Sigma-Aldrich, St. Louis, USA), rabbit anti-neuronal nuclei (NeuN, a neuronal marker, 1:500; ab128886, Abcam) at 4°C overnight. Then the sections were further incubated with the secondary antibodies Alexa Fluor 488 (goat anti-mouse IgG, 1:1000; S32354, Invitrogen, New York, USA) or Alexa Fluor 594 (donkey anti-goat (or mouse) IgG H&L, ab150132 (ab150108); Abcam) for 2 h at room temperature. All images were captured with an Olympus confocal microscope (FV1200, Olympus, Japan) and processed using FV10-ASW4.2 Viewer software. DRG and spinal cord sections with CGRP, IB4, NF200, and NeuN-positive components from each animal were counted. Data were averaged from at least eight sections/mouse, with 4 mice per group.

Fluorescence *in situ* Hybridization (FISH)

The protocol for *in situ* hybridization was adapted from previous studies [31–33]. In brief, a complementary DNA fragment of Ttyh1 (GenBank accession No. NM_021324.6, Ttyh1 nucleotides 126-1478) was cloned and riboprobes were synthesized by digoxigenin labelling.

The adult male mice were perfused with 0.01 mol/L diethylpyrocarbonate-treated phosphate-buffered saline (pH 7.4) followed by 4% formaldehyde in 0.1 mol/L phosphate buffer (pH 7.4) after deep anesthesia. The DRG and spinal cord tissues were removed and cut into 16-μm sections after cryoprotection. Then, the sections were acetylated for 10 min, pre-incubated for 1 h at 60°C, and then hybridized for 18 h at 60°C with 1 μg/mL sense or antisense DIG-labelled Ttyh1 riboprobes in hybridization buffer. Next, the hybridized sections were incubated overnight at room temperature in a mixture of peroxidase-conjugated anti-DIG antibody (Roche 11207733910, Switzerland) diluted 1:2000 and one of the following antibodies: Dy Light® 594 *Griffonia simplicifolia* lectin-IB4 (1:300; DL-1207, Vector), CGRP (goat anti-CGRP, 1:300; ab36001, Abcam), or NF200 (mouse anti-NF200, 1:300; N5389, Sigma-Aldrich).The Ttyh1 probe hybridization signal was amplified using biotinylated tyramine-glucose oxidase. After washing, the sections were incubated with a mixture of 2 μg/mL Alexa Fluor 488-conjugated streptavidin (Invitrogen) to visualize the riboprobes (Invitrogen) and 4 μg/mL Alexa Fluor 594-conjugated anti-goat, or anti-mouse IgG (Invitrogen) to visualize other molecules for 3–4 h at room temperature. Finally, the sections were coverslipped.

Quantitative Real-Time PCR (qRT-PCR)

The L3/L4 DRGs and SDHs of the lumbar enlargements were harvested under deep anesthesia. According to the manufacturer's instructions, total RNA was extracted and cDNA was reverse-transcribed. qRT-PCR was performed with SYBR (Roche). The primer pairs used for qRT-PCR were: Ttyh1 forward: 5′-CCGCGACCAAGAGTACCAG-3′, reverse: 5′-GAAGCGGATGAGGTAGACAGC-3′; β-actin forward: 5′-CATCCGTAAAGACCTCTATGC-CAAC-3′, reverse: 5′-ATGGAGCCACCGATCCACA-3′. The standard conditions were as follows: 95°C for 3 min, then 40 cycles at 95°C for 15 s, 60°C for 34 s, 95°C for 15 s, 60°C for 60 s and 95°C for 1 s for a melting curve. Relative gene expression was calculated using the $2^{-\Delta\Delta C_T}$ method. Each qRT-PCR assay was performed in triplicate.

Western Blotting

L3/L4 DRGs and SDHs of the lumbar enlargements were homogenized in ice-cold lysis buffer. The supernatant was collected by centrifugation (13000 rpm for 10 min). Protein concentration was determined by the bicinchoninic acid method. The membrane was blocked at room temperature with 5% non-fat dry milk for 2 h, and then

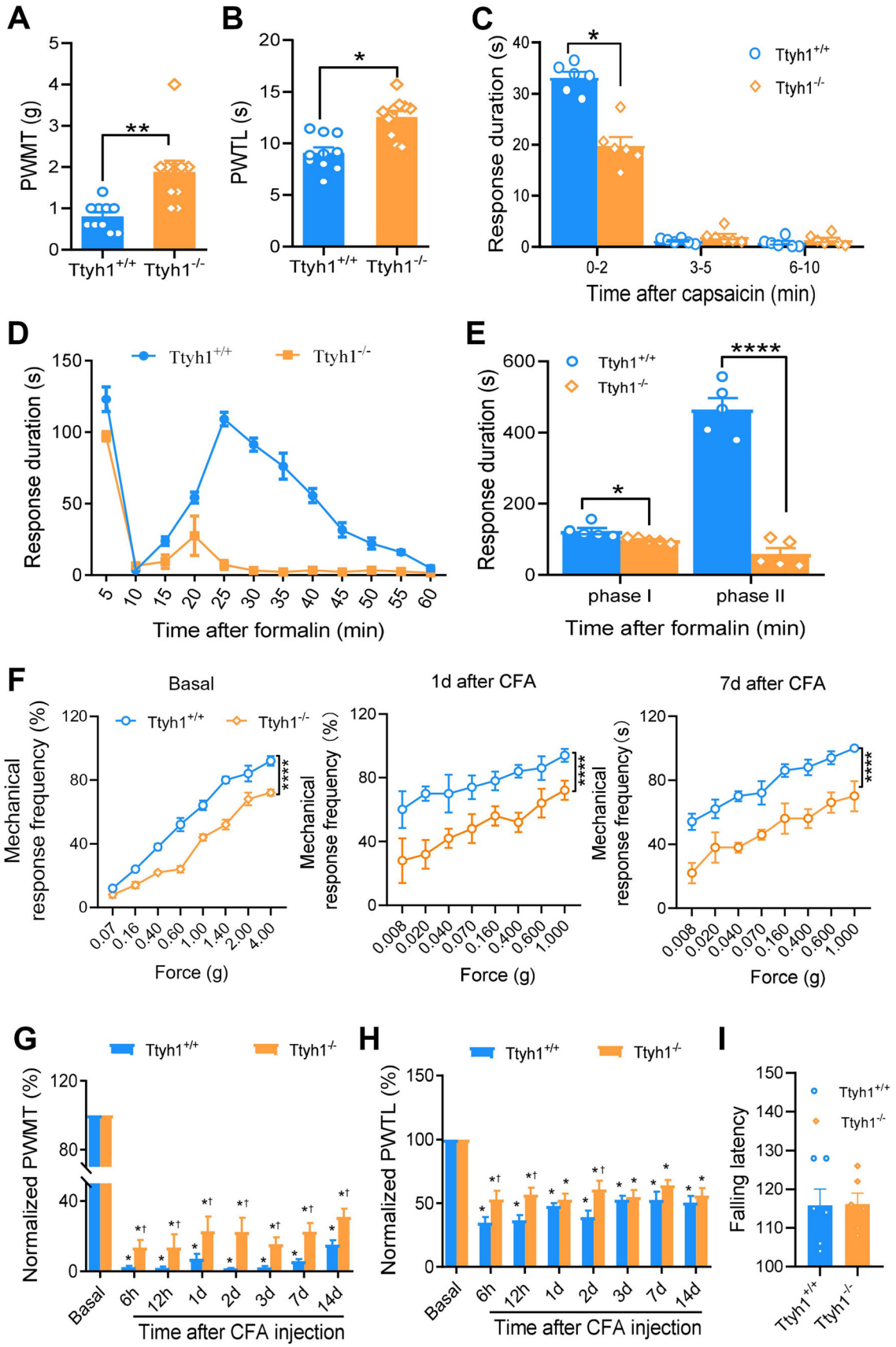
A
PWMT (g)
Ttyh1+/+
Ttyh1-/-
B
PWTL (s)
C
Response duration (s)
Time after capsaicin (min)
0-2
3-5
6-10
D
Response duration (s)
Time after formalin (min)
E
phase I
phase II
F
Basal
1d after CFA
7d after CFA
Mechanical response frequency (%)
Force (g)
G
Normalized PWMT (%)
Time after CFA injection
H
Normalized PWTL (%)
I
Falling latency

◀**Fig. 1** Deficiency of Ttyh1 attenuates the basal nociception and pain hypersensitivity associated with peripheral inflammation. **A, B** Paw withdrawal mechanical threshold (PWMT) and paw withdrawal thermal latency (PWTL) in basal pain perception (n = 10 mice). **C** Spontaneous pain induced by capsaicin (n = 6 mice). **D, E** Time course (**D**) and quantitative summary (**E**) of formalin-induced spontaneous pain (n = 5 mice). **F** Representative traces showing the response curves of basal and CFA-induced mechanical pain hypersensitivity at different time points after CFA injection (n = 10 mice). **G** Quantitative summary of the drop in PWMT to von Frey filament stimuli after CFA injection (n = 10 mice). **H** Quantitative summary of the drop in PWTL to radiant heat stimuli after CFA injection (n = 10 mice). **I** Motor function does not change with Ttyh1 deficiency ($P > 0.05$, n = 6 mice). All data are presented as mean ± SEM. $^{*}P < 0.05$, $^{**}P < 0.01$, $^{***}P < 0.001$, $^{****}P < 0.0001$, $^{\dagger}P < 0.05$ *vs* Ttyh1$^{+/+}$ mice at the same time point.

incubated with the primary antibody mouse anti-Ttyh1 (1:1000; Sigma-Aldrich) [34] overnight at 4°C. Then, the membranes were incubated at room temperature with horseradish peroxidase (HRP)-conjugated goat anti-mouse secondary antibody (1:10000; Amersham Biosciences) for 4 h, and standardized against loaded samples incubated with rabbit monoclonal anti-β-actin antibody (1:2000, Sigma-Aldrich), then incubated with HRP-conjugated goat anti-rabbit IgG (1:10000; Pierce). The membranes were incubated with enhanced chemiluminescence reagents (Pierce), and images of the membrane were analyzed. The density of the band of interest (Ttyh1) was measured and normalized to the density of the β-actin band.

Whole-Mount DRG Patch-Clamp Recording

Adult male mice (7–8 weeks old) were anesthetized with urethane (25%, 1.2 g/kg, i.p.) and L3/L4 DRGs with attached nerves were carefully removed from control mice or at 24 h following CFA injection (CFA-inflamed mice). After removing the connective tissue and capsule, the ganglia were digested in a tube containing diluted digestive enzyme solution at 37°C for 45 min and then incubated with oxygenated artificial cerebrospinal fluid (ACSF) as described in a previous study [35]. DRG neurons were identified and whole-cell current and voltage recordings were acquired. If neurons had a resting membrane potential lower than − 50 mV and exhibited overshooting action potentials, they were selected for further study.

The ACSF and intrapipette solutions were used as described previously [36]. Data were acquired with a Digidata 1550A acquisition system (Molecular Devices, CA, USA) using pCLAMP 10.6 software. Signals were low-pass filtered at 5 kHz, sampled at 10 kHz, and analyzed offline. To analyze the active membrane properties, membrane potential was held at − 60 mV under current-clamp mode. The action potential (AP) parameters were measured with depolarizing current steps (500 ms in duration and 20-pA increments). The AP threshold was determined by differentiating the AP waveform and setting a rising rate of 10 mV/ms as the inflection point of the AP. The amplitude was measured from the threshold to the spike peak, and the duration was measured at the half-width of the spike. Beyond that, a depolarizing current ramp stimulus (500 ms in duration and 50 pA increments) was also given to measure AP parameters.

DiI Labelling of Spinal Projection Neurons *in vivo* and Patch-Clamp Recordings

Male mice (3–4 weeks old) were placed in a stereotaxic apparatus after anesthetizing with pentobarbital sodium (1%, 50 mg/kg, i.p.) and received a single injection of 100 nL of 2.5% DiI into the right PAG at coordinates from the atlas of Paxinos and Watson. Two days after DiI injection, these mice received intraplantar injection of either saline (control) or CFA into the left hindpaw. One day later, transverse 350 μm–450 μm thick spinal cord slices with dorsal roots attached were cut and identified DiI-positive neurons were recorded under whole-cell patch-clamp as described elsewhere [26, 37]. The recordings were made in lamina I of the SDH through glass micropipettes with a resistance of 8 MΩ–10 MΩ. And we added QX-314 (5 mmol/L), a lidocaine derivative, into the pipette solution to prevent discharge of APs. Signals were low-pass filtered at 5 kHz, sampled at 10 kHz, and analyzed offline. The labelled neurons in lamina I were chosen to measure excitatory postsynaptic currents (EPSCs) at – 70 mV while the dorsal root was stimulated by an isolated current stimulator through a suction electrode. Test pulses of 0.1 ms with an intensity of 3 mA were given at 30-s intervals and monosynaptic C-fiber evoked EPSCs (C-eEPSCs) were recorded in the presence of the $GABA_A$ receptor antagonist gabazine (10 μmol/L; Abcam) and the glycine receptor antagonist strychnine (1 μmol/L; Sigma to block inhibitory synaptic transmission. C-fiber-evoked responses were considered to be monosynaptic with the method described in previous studies [38, 39].

C-eEPSCs were distinguished from Aδ-eEPSCs based on the conduction velocity of afferent fibers (C-fibers, < 0.8 m/s; calculated from the latency of eEPSCs to the stimulus artifact and the length of dorsal root), as described previously [38, 39]. Long-term potentiation (LTP) was induced as described in previous reports [26, 37]. Low-frequency stimulation (LFS, 2 Hz for 2 min) was applied through a dorsal root with same intensity as the test stimulation. Synaptic strength was quantified by the peak C-eEPSC amplitude.

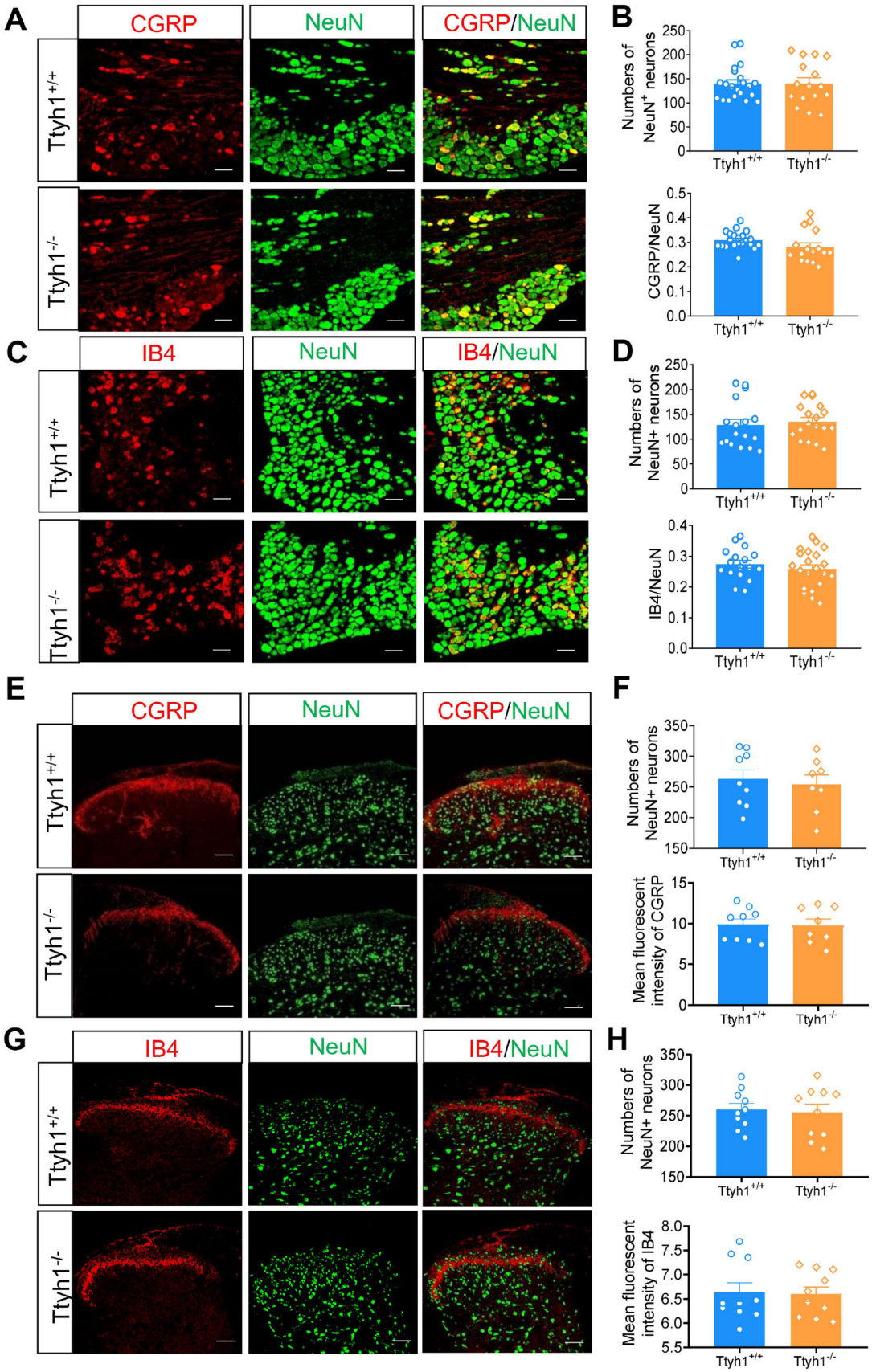
A
CGRP
NeuN
CGRP/NeuN
Ttyh1+/+
Ttyh1-/-
B
Numbers of NeuN+ neurons
CGRP/NeuN
C
IB4
NeuN
IB4/NeuN
D
Numbers of NeuN+ neurons
IB4/NeuN
E
CGRP
NeuN
CGRP/NeuN
F
Numbers of NeuN+ neurons
Mean fluorescent intensity of CGRP
G
IB4
NeuN
IB4/NeuN
H
Numbers of NeuN+ neurons
Mean fluorescent intensity of IB4

◀**Fig. 2** Deficiency of Ttyh1 has no effect on the development of nociceptive dorsal root ganglion (DRG) neurons. **A, C** Double immunofluorescence staining of DRG neurons with NeuN (green) and CGRP (red, **A**) or IB4 (red, **C**) in both Ttyh1$^{+/+}$ (**A, C**, upper panels) and Ttyh1$^{-/-}$ mice (**A, C,** lower panels). **B, D** Quantitative summary of total numbers of neurons (**B, D**, upper panels) and the ratios of CGRP-positive (**B**, lower panels) and IB4-positive (**D**, lower panels) neurons show no differences between Ttyh1$^{+/+}$ and Ttyh1$^{-/-}$ mice. **E, G** Central patterning of peptidergic (CGRP-positive) and non-peptidergic (IB4-binding) nociceptors in the spinal dorsal horn (SDH) as well as spinal intrinsic neurons (NeuN-positive) is normal in Ttyh1$^{-/-}$ mice compared to Ttyh1 $^{+/+}$ mice. **F, H** Quantitative summary showing CGRP (**F**, upper panel) and IB4 immunoreactivity (**H**, upper panel) as well as NeuN immunoreactivity (lower panel in **F** and **H**) in the SDH from Ttyh1$^{+/+}$ and Ttyh1$^{-/-}$ mice. All data are presented as mean ± SEM. Scale bars, 50 μm; n = 4 mice per group.

In a subset of experiments, the dorsal root was stimulated with paired pulses at an inter-stimulus interval of 110 ms (0.1 ms pulse duration, 3 mA intensity, every 30 s). The paired-pulse ratio (facilitation or depression) of C-eEPSCs was calculated as the value of the second C-eEPSC divided by that of the first C-eEPSCs in a pair. In another subset of experiments, miniature EPSCs (mEPSCs) were recorded at a holding potential of – 70 mV after inhibitory synaptic transmission was blocked by gabazine (10 μmol/L) and strychnine (1 μmol/L), as well as tetrodotoxin (0.5 μmol/L; Sigma) to block Na^+ channels.

Nociceptor-Specific Knockdown of Ttyh1

Nociceptor-specific knockdown of Ttyh1 was achieved with the methods described previously [40]. Briefly, based on the cDNA sequence of mouse Ttyh1, we generated oligonucleotides corresponding to Ttyh1-specific shRNA, and annealed and cloned them into an AAV2/8 plasmid that was designed with a floxed enhanced green fluorescent protein (EGFP)-tagged stop sequence (rAAV2/8-Efla-mCherry-U6-Loxp-CMV-EGFP-Loxp-shRNA Ttyh1) (Fig. 7A, B). Similarly, a control shRNA (rAAV2/8-Efla-mCherry-U6-Loxp-CMV-EGFP-Loxp) was cloned and packaged (scrambled AAV-shRNA) to serve as a negative control for potential non-specific effects associated with the delivery of shRNA. To accomplish nociceptor-specific knockdown of Ttyh1, loxp-Ttyh1 shRNA-expressing AAV2/8 (AAV-shRNA Ttyh1) or scrambled AAV-shRNA (1.0 μL) was injected into the L3/L4 DRGs of SNS-Cre mice. Scramble AAV-shRNA was injected in a manner similar to that used for controls.

Data Analysis and Statistics

All data are presented as mean ± SEM). For comparisons of multiple groups, two-way or one-way analysis of variance (ANOVA) with random measures was performed followed by *post-hoc* Fisher's test to determine statistically significant differences. When comparing two groups of parallel studies, Student's t-test was used. $P < 0.05$ was considered significant.

Results

Ttyh1 Deficiency Attenuates Basal Nociception and Pain Hypersensitivity Associated with Peripheral Inflammation

To investigate the specific role of Ttyh1 in pain regulation, we tested basal nociception and inflammatory pain hypersensitivity in male Ttyh1-knockout (Ttyh1$^{-/-}$) and wild-type (Ttyh1$^{+/+}$) mice. We first compared basal mechanical and thermal sensitivity. Compared with Ttyh1$^{+/+}$ mice, Ttyh1$^{-/-}$ mice displayed blunted responses to mechanical (Fig. 1A) and thermal stimuli (Fig. 1B). Acute nocifensive responses induced by intraplantar injection of capsaicin were attenuated by deletion of Ttyh1 (Fig. 1C) as well. These results indicate that Ttyh1 is required for the nociceptive behavior in response to acute noxious stimuli.

Next, we addressed whether Ttyh1 is involved in the development of pathological pain. First, we focused on a formalin-induced pain model that is associated with persistent spontaneous pain [41]. Formalin induced a biphasic spontaneous nociceptive response in Ttyh1$^{+/+}$ mice, including an initial robust phase in which the lifting, licking, and flinching of the paws were recorded for the first 5 min (phase I). This was followed by a brief decline in these behaviors, and then a second phase of 30 min–60 min (phase II) (Fig. 1D, E). Analysis of the time that the mice spent on these spontaneous behaviors showed that the formalin-induced spontaneous pain responses of Ttyh1$^{-/-}$ mice, compared to those of Ttyh1$^{+/+}$ mice, were significantly reduced in both phases, with an especially prominent reduction in phase II (Fig. 1D, E). This suggests a pivotal role of Ttyh1 in the persistent spontaneous nociception produced by noxious irritation.

A model of chronic inflammatory pain (unilateral hindpaw inflammation induced by injection of CFA) was used in the next study, because this model is associated with primary hyperalgesia and allodynia [26]. Von Frey mechanical and radiant heat stimuli were applied to the ipsilateral paw to assess sensory hypersensitivity at the basal levels and 6 h, 12 h, and 1, 2, 3, 7, and 14 days after peripheral inflammation. Consistent with the above, the basal stimulus-response curve revealed a mild hyposensitivity to mechanical stimuli in Ttyh1$^{-/-}$ mice compared to that in Ttyh1$^{+/+}$ mice (Fig. 1F, left panel). After CFA injection, compared to the basal curve, the stimulus-response curve of Ttyh1$^{+/+}$ mice showed a characteristic

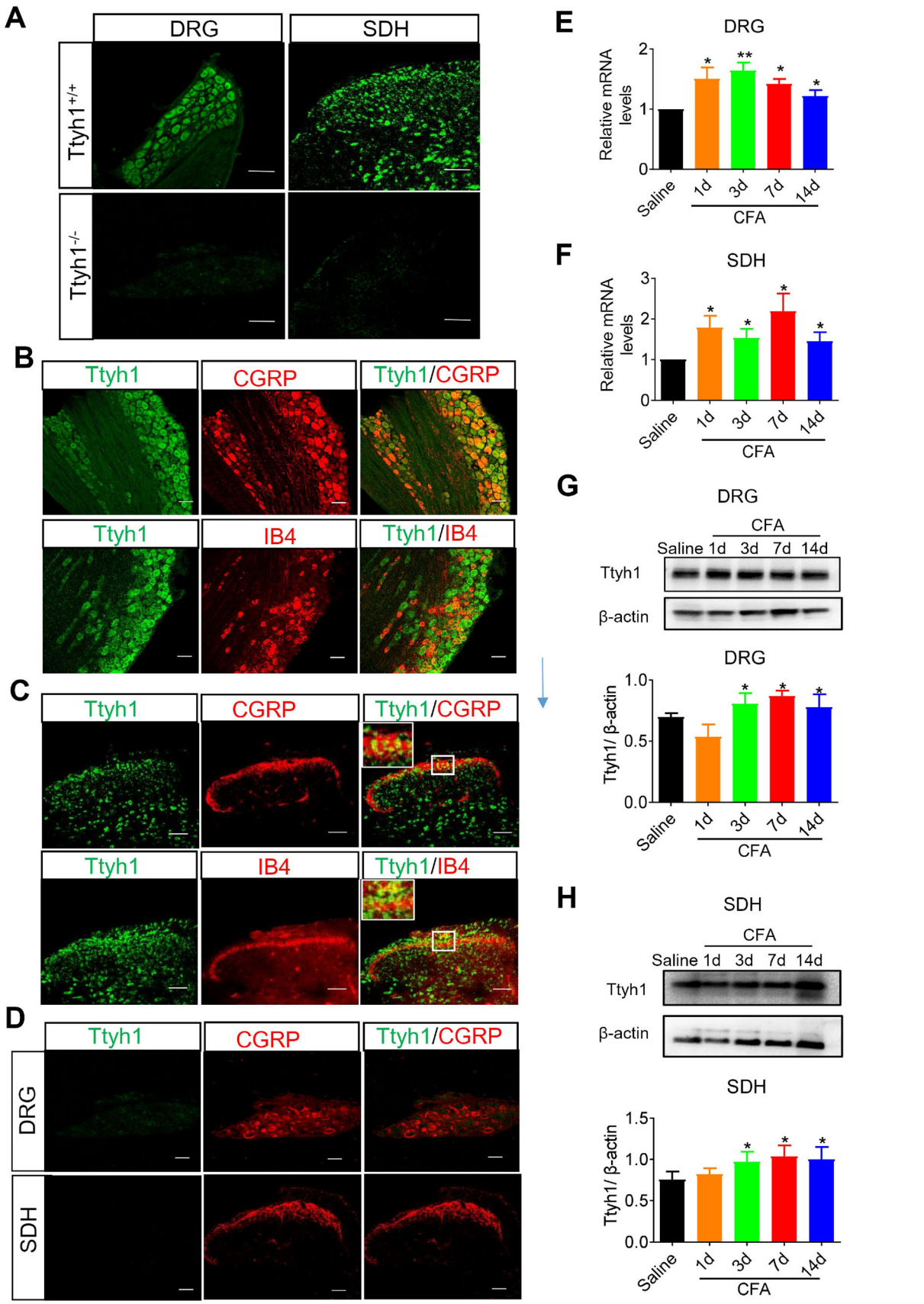
A
DRG
SDH
Ttyh1+/+
Ttyh1-/-
B
Ttyh1
CGRP
Ttyh1/CGRP
Ttyh1
IB4
Ttyh1/IB4
C
Ttyh1
CGRP
Ttyh1/CGRP
Ttyh1
IB4
Ttyh1/IB4
D
Ttyh1
CGRP
Ttyh1/CGRP
DRG
SDH
E
DRG
Relative mRNA levels
Saline
1d
3d
7d
14d
CFA
F
SDH
Relative mRNA levels
Saline
1d
3d
7d
14d
CFA
G
DRG
CFA
Saline 1d 3d 7d 14d
Ttyh1
β-actin
DRG
Ttyh1/ β-actin
Saline
1d
3d
7d
14d
CFA
H
SDH
CFA
Saline 1d 3d 7d 14d
Ttyh1
β-actin
SDH
Ttyh1/ β-actin
Saline
1d
3d
7d
14d
CFA

◀**Fig. 3** The expression and upregulation of Ttyh1 in the dorsal root ganglion (DRG) and spinal dorsal horn (SDH) following peripheral inflammation. **A** Fluorescence *in situ* hybridization of Ttyh1 (green) in DRG neurons and SDH neurons (n = 3 mice). **B** Double immunofluorescence staining of Ttyh1 (green) with CGRP (red, upper panels) or IB4 (red, lower panels) in the DRG (n = 6 mice). **C** Double immunofluorescence staining of Ttyh1 (green) with CGRP (red, upper panels) or IB4 (red, lower panels) in the SDH (n = 6 mice). **D** Double immunofluorescence staining of Ttyh1 (green) with CGRP (red) in the DRG (upper panels) and SDH (lower panels) in Ttyh$^{-/-}$ mice (n = 6 mice). **E, F** Upregulation of Ttyh1 at the mRNA level in the DRG (**E**) and SDH (**F**) at different time points following peripheral CFA inflammation (n = 5 mice). **G, H** Typical examples and quantitative summary showing upregulation of Ttyh1 at the protein level in the DRG (**G**) and SDH (**H**) at different time points following CFA injection (n = 8 mice). All data are presented as mean ± SEM. *$P < 0.05$, **$P < 0.01$. Scale bars, 50 μm.

leftward and upward shift, which reflects mechanical hypersensitivity (blue circles in Fig. 1F). In contrast, the stimulus-response curve of Ttyh1$^{-/-}$ mice demonstrated a small deviation from the basal curve under CFA inflammation (orange circles in Fig. 1F). When standardized to their corresponding baseline levels, the relative decrease in response to von Frey hairs in the inflamed state over the basal state was significantly lower in Ttyh1$^{-/-}$ mice than in Ttyh1$^{+/+}$ mice (Fig. 1G). Furthermore, the degree of thermal hyperalgesia in Ttyh1$^{-/-}$ mice was significantly lower than in Ttyh1$^{+/+}$ mice at 6 h, 12 h, and 2 days after CFA inflammation, while at other time points, the degree of thermal hyperalgesia did not significantly differ between Ttyh1$^{-/-}$ and Ttyh1$^{+/+}$ mice (Fig. 1H). In contrast to the dramatic effect of Ttyh1 on pain sensation, motor coordination was not altered by deletion of Ttyh1 (Fig. 1I). Thus, it may be inferred from the above that Ttyh1 plays a crucial role in the development of the primary hyperalgesia and allodynia associated with tissue inflammation.

To determine whether deletion of Ttyh1 induces aberrant developmental defects in sensory neurons, we quantified the number of DRG neurons and SDH neurons in adult Ttyh1$^{+/+}$ and Ttyh1$^{-/-}$ mice. The number of DRG neurons labelled by NeuN was not altered by deletion of Ttyh1 (Fig. 2A–D). Detailed analysis of different populations of nociceptive DRG neurons revealed that the percentages of CGRP-expressing peptidergic DRG neurons and IB4-labelled non-peptidergic DRG neurons were comparable between adult Ttyh1$^{+/+}$ and Ttyh1$^{-/-}$ mice (Fig. 2A, B for CGRP-positive DRG neurons, Fig. 2C, D for IB4-positive DRG neurons). Furthermore, immunostaining for CGRP and binding to IB4 in the SDH revealed that the central patterning of peptidergic and non-peptidergic nociceptors was normal in adult Ttyh1$^{-/-}$ mice (Fig. 2E, F for CGRP-expressing central terminals, Fig. 2G, H for IB4-binding central terminals). Meanwhile, the number of SDH neurons was unaltered by deletion of Ttyh1 (Fig. 2E–H). Taken together, we conclude from the above that the deficit of pain hypersensitivity in adult Ttyh1$^{-/-}$ mice is not due to developmental defects in peripheral sensory and SDH neurons, and this enables us to further explore its underlying mechanisms in pain sensitization.

Ttyh1 is Expressed in the DRG and SDH and is Upregulated Following Peripheral Inflammation

We employed several different approaches to examine the expression of Ttyh1 and its changes in the DRG and SDH in basal and inflammatory pain states. We used FISH to examine the expression patterns of Ttyh1 in DRG and SDH. *In situ* hybridization with probes targeting the mRNA of Ttyh1 yielded specific signals in Ttyh1$^{+/+}$ mice, but not in Ttyh1$^{-/-}$ mice, showing the specificity of the probe (Fig. 3A). To further delineate the expression profile of Ttyh1, we examined the co-localization of different markers for DRG neurons with Ttyh1 at the mRNA level (FISH with the Ttyh1 probe). FISH analysis revealed that Ttyh1 was expressed in nearly all DRG neurons including CGRP-expressing peptidergic nociceptors and IB4-labelled non-peptidergic nociceptors (Fig. 3B). In addition, we observed dense expression of Ttyh1 in the SDH, including co-localization with CGRP-expressing and IB4-binding central terminals as well as expression in the intrinsic SDH neurons (Fig. 3C). We also detected co-labeling of Ttyh1 and CGRP in the DRG and SDH of Ttyh1$^{-/-}$ mice, and no expression of green fluorescent-labeled Ttyh1 (Fig. 3D). These results indicate that Ttyh1 is broadly expressed in the DRG and SDH where the first-order neurons and the first synapse are located in the nociceptive pathway.

We next sought to assess the changes of Ttyh1 expression in chronic inflammatory pain states. The qRT-PCR analysis revealed a significant and persistent upregulation of Ttyh1 at the mRNA level in the ipsilateral L3–L4 DRGs and SDH in the lumbar enlargement at 1, 3, 7, and 14 days following CFA inflammation (Fig. 3E for DRG, and Fig. 3F for SDH). Consistent with this, Western blotting showed increased expression of Ttyh1 at the protein level in L3-L4 DRGs (Fig. 3G). A similar trend for Ttyh1 expression changes at the protein level was also found in the SDH upon CFA inflammation (Fig. 3H). In summary, these results indicate a wide expression of Ttyh1 in the DRG and SDH, which is the first and important gate in the nociceptive pathway, and significant and persistent plastic changes of expression in response to peripheral inflammation.

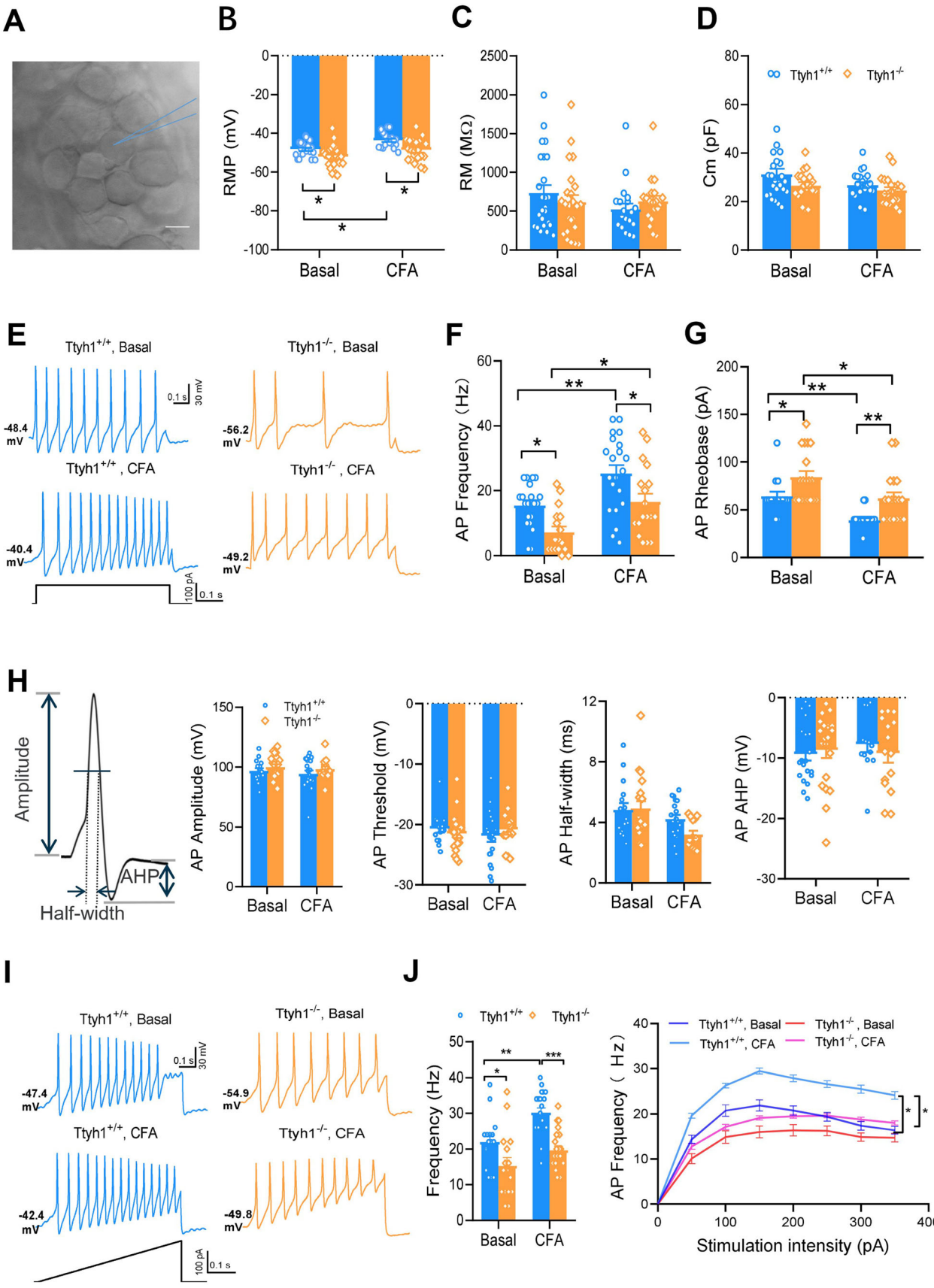
A
B
C
D
RMP (mV)
RM (MΩ)
Cm (pF)
Basal
CFA
Ttyh1+/+
Ttyh1-/-
E
Ttyh1+/+, Basal
Ttyh1-/-, Basal
Ttyh1+/+ , CFA
Ttyh1-/- , CFA
-48.4 mV
-56.2 mV
-40.4 mV
-49.2 mV
0.1 s
30 mV
100 pA
F
G
AP Frequency (Hz)
AP Rheobase (pA)
H
Amplitude
AHP
Half-width
AP Amplitude (mV)
AP Threshold (mV)
AP Half-width (ms)
AP AHP (mV)
I
J
Ttyh1+/+, Basal
Ttyh1-/-, Basal
Ttyh1+/+, CFA
Ttyh1-/-, CFA
-47.4 mV
-54.9 mV
-42.4 mV
-49.8 mV
Frequency (Hz)
AP Frequency (Hz)
Stimulation intensity (pA)

◀**Fig. 4** Excitability of small dorsal root ganglion (DRG) neurons is substantially reduced in Ttyh1$^{-/-}$ mice in both basal and inflamed states. **A** Image of recording from a small DRG neuron in a whole-mount DRG preparation. **B–D** Passive membrane properties including RMP (**B**), Rm (**C**), and Cm (**D**) of small DRG neurons from Ttyh1$^{+/+}$ and Ttyh1$^{-/-}$ mice in both basal and CFA-inflamed states. **E** Representative traces showing spike firing in response to a depolarizing current step in small DRG neurons from Ttyh1$^{+/+}$ and Ttyh1$^{-/-}$ mice in both basal and CFA-inflamed states. **F, G** Quantitative analysis showing that deletion of Ttyh1 attenuates the firing frequency (**F**) and increases rheobase (**G**) in small DRG neurons in both basal and inflamed states. **H** Other parameters such as AP amplitude, threshold, and half-width as well as after hyperpolarization (AHP) remain intact in the two genotypes in both basal and CFA groups. **I** Typical traces showing spike firing in response to ramp current injection in small DRG neurons from Ttyh1$^{+/+}$ and Ttyh1$^{-/-}$ mice in both basal and CFA-inflamed states. **J** Quantitative summary showing the firing frequency induced by ramp current injection at 100 pA (left panel) and the input (stimulation intensity)-output (AP frequency) (I–O) curve induced by ramp current injection from Ttyh1$^{+/+}$ and Ttyh1$^{-/-}$ mice in both basal and inflamed states. All data are presented as mean ± SEM. $^{*}P < 0.05$, $^{**}P < 0.01$, $^{***}P < 0.001$. Scale bar, 10 μm.

Excitability of Nociceptive DRG Neurons is Substantially Reduced in Ttyh1$^{-/-}$ Mice

To determine the cellular and molecular mechanisms by which Ttyh1 regulates pain, we first made patch-clamp recordings from small-diameter nociceptive DRG neurons (≤ 20 μm) in whole-mount DRG preparations from Ttyh1$^{+/+}$ and Ttyh1$^{-/-}$ mice (Fig. 4A). The passive membrane properties including resting membrane potential (RMP), membrane resistance (Rm), and membrane capacitance (Cm) were compared between the two genotypes in both basal and CFA-inflamed groups. In the basal state, small DRG neurons in Ttyh1$^{-/-}$ mice had a more negative RMP than their littermate controls (Fig. 4B), indicating its role in determining RMP. Upon CFA inflammation, small DRG neurons from Ttyh1$^{+/+}$ mice showed a significant shift to the depolarizing direction in RMP (Fig. 4B), which did not occur in those from Ttyh1$^{-/-}$ mice (Fig. 4B). The other two parameters, Rm and Cm, were comparable in the two genotypes in either the basal or CFA-inflamed state (Fig. 4C, D). More importantly, the active membrane properties of nociceptive DRG neurons were significantly different between Ttyh1$^{+/+}$ and Ttyh1$^{-/-}$ mice in both basal and CFA-inflamed states. For example, small DRG neurons from Ttyh1$^{-/-}$ mice, compared to Ttyh1$^{+/+}$ mice, had a lower firing frequency evoked by a depolarizing current step and higher rheobase required to evoke an AP (Fig. 4E). Upon CFA inflammation, Ttyh1$^{+/+}$ DRG neurons displayed dramatic hyperexcitability, as characterized by increased firing frequency and lowered rheobase (Fig. 4E–G). In contrast, the magnitude of this hyperexcitability driven by inflammation was much attenuated in Ttyh1$^{-/-}$ DRG neurons, although they also became hyperexcitable to some degree after inflammation (Fig. 4E–G). The other parameters such as AP threshold, amplitude, and half-width as well as after hyperpolarization remained intact between the two genotypes in both the basal and CFA groups (Fig. 4H). These data suggest that Ttyh1 plays a pivotal role in the regulation of nociceptor excitability. This inference was further supported by a ramp current injection protocol, which revealed that the excitability of small DRG neurons from Ttyh1$^{-/-}$ mice in both the basal and CFA-inflamed states was much lower than that from littermate controls (Fig. 4I, J). The input (stimulation intensity)-output (AP frequency) curves of small DRG neurons from Ttyh1$^{-/-}$ mice were shifted downward compared to those from littermate controls both in the basal and inflamed states (Fig. 4J).

Silencing Ttyh1 Eliminates Spinal Synaptic Transmission and Activity-Dependent Plasticity

Considering the crucial role of Ttyh1 in nociceptor excitability, we next tested whether Ttyh1 is involved in excitatory synaptic transmission and activity-dependent synaptic plasticity at the synapses between nociceptive primary afferents and spinal lamina I projection neurons. Since the synaptic LTP between C-nociceptors and spinal-PAG projection neurons in lamina I is considered to be a cellular basis for chronic pain [25–27], in the preparation of spinal cord slices attached with dorsal root attached, we recorded C-eEPSCs on spinal-PAG projection neurons that were retrogradely labelled by stereotactic injection of DiI into the PAG (Fig. 5A, B). Electrical stimulation of the dorsal root at 3 mA is sufficient to fully activate C-fibers [25, 26], and monosynaptic C-eEPSCs in lamina I spinal-PAG projection neurons were recorded at a holding potential of – 70 mV in the presence of the antagonists of inhibitory synaptic transmission, gabazine (10 μmol/L) and strychnine (1 μmol/L). Excitatory synaptic transmission was analyzed by constructing detailed input (dorsal root stimulation intensity)-output (eEPSC amplitude) curves of C-eEPSCs in both genotypes from basal and CFA groups. As shown in Fig. 5C, D, Ttyh1$^{-/-}$ mice showed a reduced basal excitatory synaptic transmission, characterized by a mild downward shift of the input-output curve (I-O curve), compared to Ttyh1$^{+/+}$ mice in the basal state. At 24 h post-CFA inflammation, spinal-PAG projection neurons from Ttyh1$^{+/+}$ mice displayed dramatic synaptic potentiation, represented by as a leftward and upward shift in the I–O curve of C-eEPSCs and increased magnitude of C-eEPSCs compared with the basal state (Fig. 5E, F). In striking contrast, the magnitude of this synaptic potentiation evoked by CFA was largely reduced

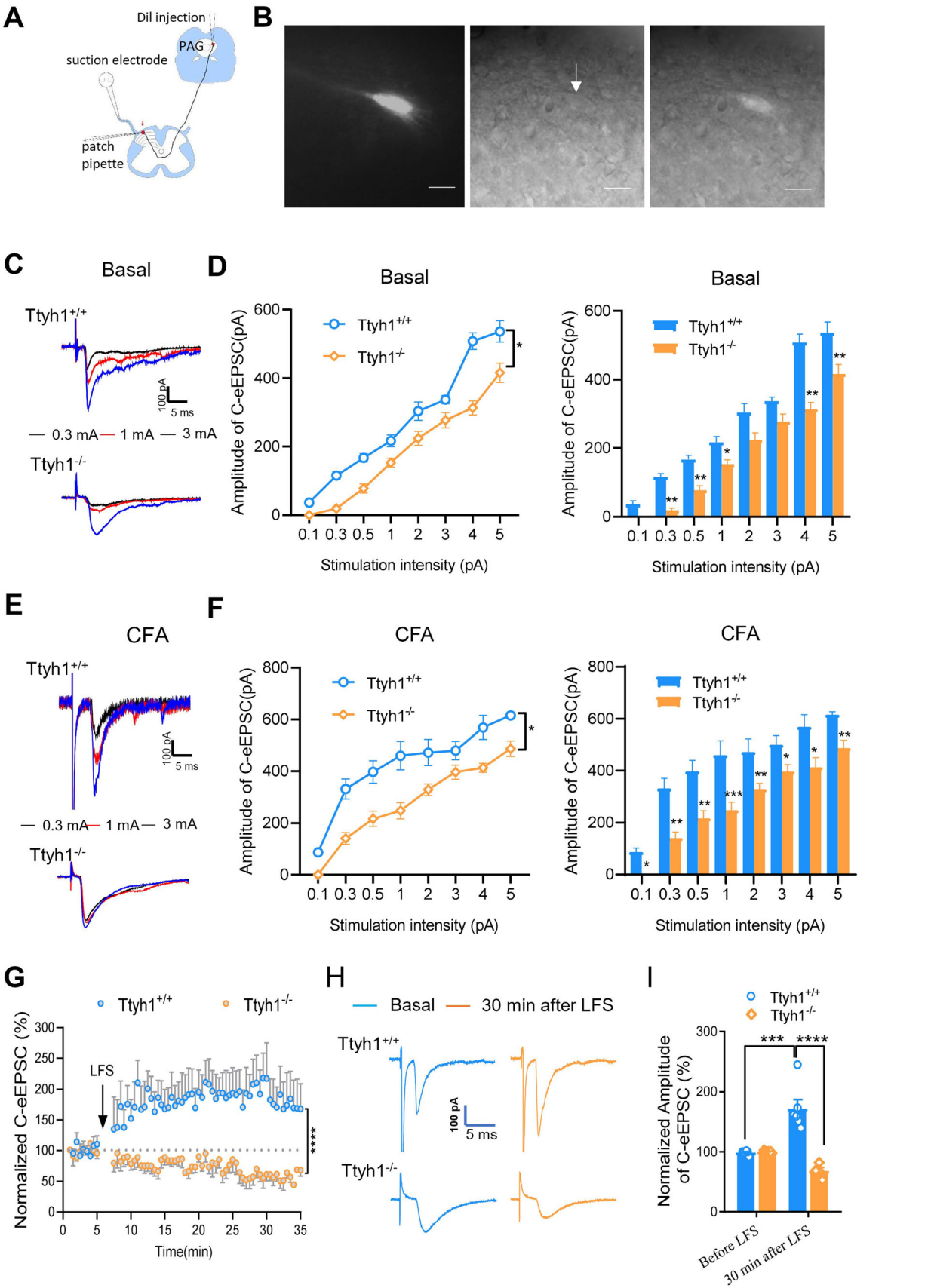
A
Dil injection
PAG
suction electrode
patch pipette
B
C
Basal
Ttyh1+/+
100 pA
5 ms
0.3 mA 1 mA 3 mA
Ttyh1-/-
D
Basal
Amplitude of C-eEPSC(pA)
Ttyh1+/+
Ttyh1-/-
Stimulation intensity (pA)
E
CFA
F
CFA
G
Normalized C-eEPSC (%)
LFS
Time(min)
H
Basal
30 min after LFS
I
Normalized Amplitude of C-eEPSC (%)
Before LFS
30 min after LFS

◀**Fig. 5** Deficiency of Ttyh1 eliminates spinal synaptic transmission and activity-dependent plasticity. **A** Schematic of whole-cell patch-clamp recording from spinal-PAG projection neurons. **B** Photographs showing DiI-labeled spinal-PAG projection neurons under fluorescent (left panel), transmission (middle panel), and merged modes (right panel). **C, E** Representative traces showing C-eEPSCs recorded from $Ttyh1^{+/+}$ and $Ttyh1^{-/-}$ mice in basal (**C**) and CFA-inflamed (**E**) states. **D, F** Quantitative analysis of the input-output curves of C-eEPSCs from $Ttyh1^{+/+}$ and $Ttyh1^{-/-}$ mice in basal (**D**) and CFA-inflamed (**F**) state. **G–I** Time course (**G**), typical examples (**H**), and quantitative summary (**I**) of synaptic LTP induced by low-frequency conditioning stimulation (LFS) (2 Hz, 2 min, 3 mA) in $Ttyh1^{+/+}$ and $Ttyh1^{-/-}$ mice. All data are presented as mean ± SEM. $^{*}P < 0.05$, $^{**}P < 0.01$, $^{***}P < 0.001$, $^{****}P < 0.0001$. Scale bars, 10 μm.

in $Ttyh1^{-/-}$ mice, although they were also potentiated to some degree after inflammation (Fig. 5C, E).

To further ascertain the crucial role of Ttyh1 in spinal synaptic potentiation, we then assessed the LTP induced by conditioning electrical stimuli which mimics natural, asynchronous low-rate discharges in C-nociceptors under pathological states [36]. In spinal-PAG projection neurons of $Ttyh1^{+/+}$ mice, conditioning LFS at 2 Hz for 2 min (3 mA) produced LTP of monosynaptic C-eEPSCs by $> 200\%$ at 30 min (Fig. 5G–I). In striking contrast to $Ttyh1^{+/+}$ mice, the same conditioning stimuli did not evoke LTP in spinal-PAG projection neurons in $Ttyh1^{-/-}$ mice and even led to long-term depression (LTD) of C-eEPSCs to $< 70\%$ at 30 min (Fig. 5G–I). In conclusion, these results collectively suggest that Ttyh1 is a key determinant of spinal nociceptive transmission and activity-dependent synaptic plasticity at the first synapse of the pain circuits.

Ttyh1 Increases Synaptic Transmission *via* Presynaptic Mechanisms

To address the relative contributions of presynaptic and postsynaptic mechanisms in the modulation of synaptic transmission and plasticity by Ttyh1, we first analyzed mEPSCs. As illustrated in Fig. 6A, deletion of Ttyh1 significantly reduced the frequency of mEPSCs recorded in spinal-PAG projection neurons (Fig. 6A, B, D). In contrast, the amplitude of mEPSCs was comparable in spinal-PAG projection neurons from $Ttyh1^{+/+}$ and $Ttyh1^{-/-}$ mice (Fig. 6A, C, E). Analysis of the cumulative distribution of inter-event intervals and mEPSC amplitudes for 2 min showed 874.2 ± 113.3 and 530.6 ± 58.9 events in the $Ttyh1^{+/+}$ and $Ttyh1^{-/-}$ mice, respectively. This showed that deficiency of Ttyh1 increased the proportion of mESPCs with longer inter-event intervals (Fig. 6B), but was without any effect on the cumulative distribution of mEPSC amplitude (Fig. 6C). These data infer that Ttyh1 enhances synaptic transmission *via* a presynaptic mechanism. Because mEPSC frequency is associated with glutamate release from not only the central terminals of primary afferents but also glutamatergic interneuron terminals in the SDH, we could not dissect the role of presynaptic Ttyh1 from nociceptor terminals with mEPSC analysis.

To further confirm the specific role of presynaptic Ttyh1 from nociceptor terminals, we further analyzed the paired-pulse ratio (PPR), which represents a transient increase or decrease in the second eEPSC shortly after the first eEPSC, and is considered to be a sign of presynaptic mechanisms of LTP [42]. As we reported previously [26, 43], both paired-pulse facilitation (PPF) and paired-pulse depression (PPD) can be recorded in spinal neurons. For example, we found that ∼ 52.8% of spinal-PAG projection neurons displayed PPF, while the other 47.2% displayed PPD [43]. In spinal slices from $Ttyh1^{+/+}$ and $Ttyh1^{-/-}$ mice, we analyzed the PPR for the basal state and 30 min after LFS. Compared to $Ttyh1^{+/+}$ mice, the PPF was significantly reduced in $Ttyh1^{-/-}$ mice in the basal state and the PPF of $Ttyh1^{+/+}$ mice was significantly changed after LFS, but not that of $Ttyh1^{-/-}$ mice (Fig. 6F, G). In addition, PPD did not change in both the basal state and 30 min after LFS in the two genotypes (Fig. 6H, I). These data indicate a presynaptic origin of Ttyh1 action. In conclusion, mEPSCs and PPR analyses collectively strengthened the idea that Ttyh1 enhances spinal synaptic transmission *via* a presynaptic mechanism involving an increase in release probability from presynaptic nociceptor terminals.

Nociceptor-Specific Deficiency of Ttyh1 Eliminates Basal Nociception and Pain Hypersensitivity Caused by Peripheral Inflammation

Given the pivotal role of Ttyh1 expressed in nociceptors in the mediation of nociceptor hyperexcitability and spinal synaptic potentiation, we went on to dissect the relative contribution of Ttyh1 localized in nociceptors to the development of pain hypersensitivity upon inflammation. To this end, we selectively eliminated Ttyh1 expression by Cre-loxP deletion of the Ttyh1 gene in nociceptors *via* injection of loxP-Ttyh1 shRNA-expressing AAV2/8 into the L3–L4 DRGs of SNS-Cre mice (Fig. 7A, B). As described previously, SNS-Cre mice under the control of the Nav1.8 promoter can achieve conditional gene deletion specifically in nociceptive DRG neurons expressing Nav1.8, while expression in the central nervous system and non-neuronal cells is preserved [26, 44]. Western blot analysis confirmed a nociceptor-specific loss of Ttyh1 by this virion strategy (Fig. 7C, D). Analysis of acute withdrawal responses to paw pressure and thermal stimuli revealed that mice expressing AAV2/8-shRNA Ttyh1 in nociceptors exhibited blunted responses in comparison

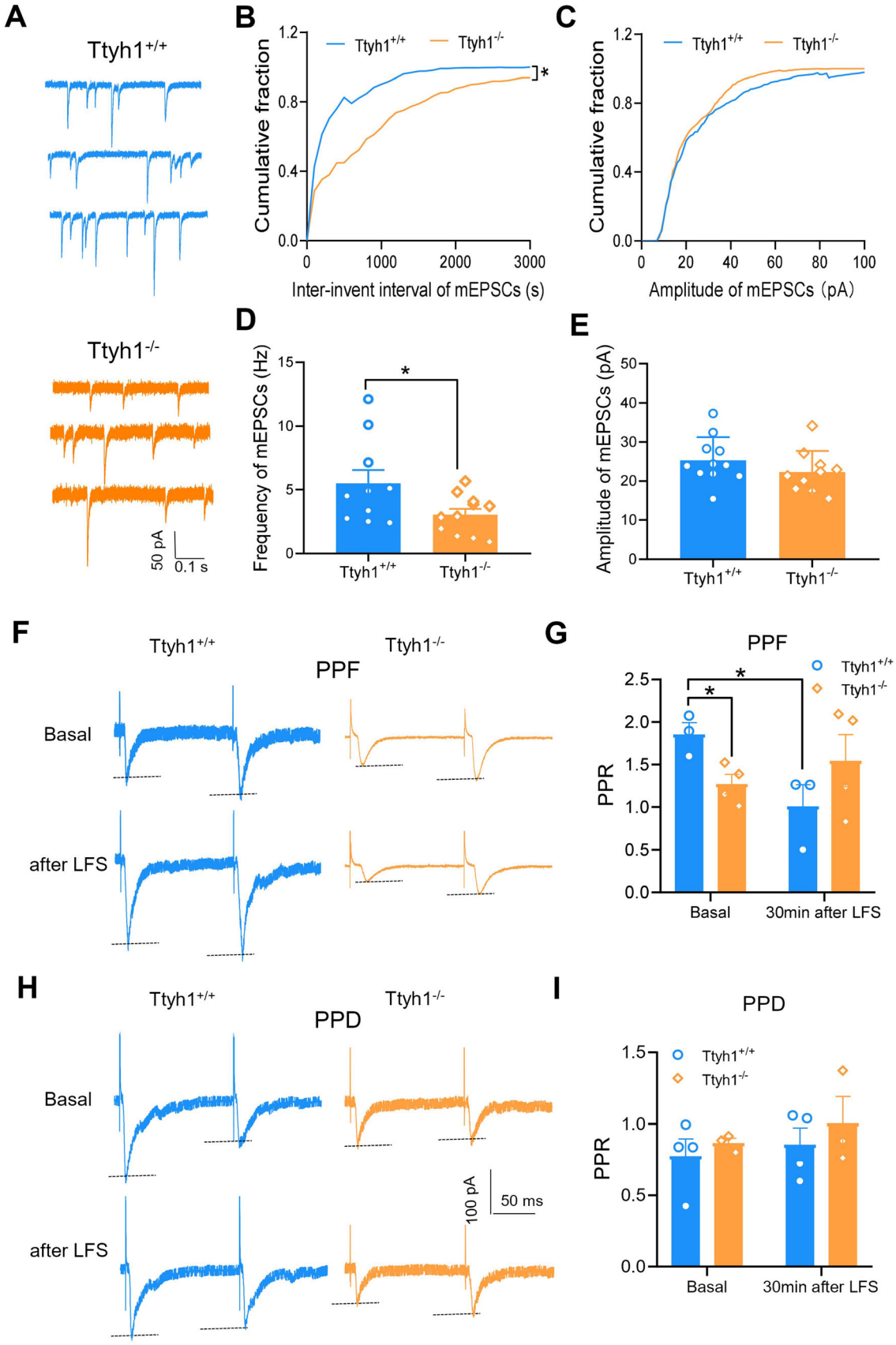
A
Ttyh1+/+
Ttyh1-/-
50 pA
0.1 s
B
Cumulative fraction
Ttyh1+/+
Ttyh1-/-
*
Inter-invent interval of mEPSCs (s)
C
Cumulative fraction
Ttyh1+/+
Ttyh1-/-
Amplitude of mEPSCs (pA)
D
Frequency of mEPSCs (Hz)
*
Ttyh1+/+
Ttyh1-/-
E
Amplitude of mEPSCs (pA)
Ttyh1+/+
Ttyh1-/-
F
Ttyh1+/+
Ttyh1-/-
PPF
Basal
after LFS
G
PPF
Ttyh1+/+
Ttyh1-/-
PPR
Basal
30min after LFS
H
Ttyh1+/+
Ttyh1-/-
PPD
Basal
after LFS
100 pA
50 ms
I
PPD
Ttyh1+/+
Ttyh1-/-
PPR
Basal
30min after LFS

◀**Fig. 6** Ttyh1 increases synaptic transmission *via* presynaptic mechanisms. **A–E** Analysis of the frequency and amplitude of mEPSCs from Ttyh1$^{+/+}$ and Ttyh1$^{-/-}$ mice. Typical traces of mEPSCs from both genotypes (**A**), cumulative curves and quantitative summary for mEPSC frequency (**B, D**) and for mEPSC amplitude (**C, E**). **F–I** Analysis of paired-pulse facilitation (PPF) and paired-pulse depression (PPD) of C-eEPSCs induced by pairs of stimuli at an interstimulus interval of 110 ms in spinal-PAG projection neurons from Ttyh1$^{+/+}$ and Ttyh1$^{-/-}$ mice. Typical examples of PPF and PPD prior to and at 30 min after LFS from both genotypes (**F**, **H**) and quantitative summary of the changes in PPF and PPD after LFS in both genotypes (**G**, **I**). All data are presented as mean ± SEM. $^{*}P < 0.05$.

with those expressing AAV2/8-conRNA (scrambled shRNA) (Fig. 7E–H), similar to global Ttyh1$^{-/-}$ mice. In the context of CFA-induced chronic inflammatory pain, mice expressing AAV2/8-conRNA displayed dramatic mechanical hyperalgesia and allodynia as well as thermal hyperalgesia at 1, 3, and 7 days after inflammation (Fig. 7E–H). In striking contrast, the magnitude of this pain hypersensitivity was greatly alleviated by nociceptor-specific knockdown of Ttyh1 (Fig. 7E–H). We can thus conclude from the above that Ttyh1 expressed in nociceptors is a key determinant of pain sensitization. Targeting Ttyh1 in nociceptors may represent a potential therapeutic strategy with few side-effects.

Discussion

Ttyh1 is a Critical Mediator of Pain Detection and Sensitization Following Peripheral Inflammation

The novel and most important findings of this study are that we identified Ttyh1 for the first time as a critical mediator of basal nociception and pain sensitization during the course of chronic inflammatory pain. Previous studies have shown that Ttyh1 is mainly restricted to neural tissue ranging from the embryonic stage to adulthood and from neurons to glial cells [17, 22, 45]. Thus, Ttyh1 has been implicated in a variety of neurological diseases and disorders including epilepsy, early embryonic development, and brain tumors [13, 17–22]. Recent studies reported that Ttyh1 regulates embryonic neural stem cell properties *via* reciprocal interaction with the Notch signaling pathway [21, 46]. Other studies revealed dramatic upregulation and the active involvement of Ttyh1 during epileptogenesis and epilepsy [18, 19]. Fusion of Ttyh1 with the C19MC microRNA cluster was shown to underlie embryonal brain tumor with multilayered rosette through driving the expression of a brain-specific DNA methyltransferase DNMT3B isoform [20]. However, little is known about the role of Ttyh1 in sensory systems although qRT-PCR and *in situ* hybridization analysis revealed the expression of Ttyh1 in the DRG and spinal cord [22, 24]. In the present study, we systemically examined the expression profile and plastic changes of Ttyh1 in pain circuits at the DRG and spinal levels and its functional role in pain detection and sensitization. Our analysis demonstrated that Ttyh1 is extensively expressed in CGRP-expressing peptidergic and IB4-binding non-peptidergic nociceptive DRG neurons and their presynaptic central terminals in the SDH. Upon peripheral inflammation, Ttyh1 exhibited dramatic upregulation at both the mRNA and protein levels in the DRG and SDH. Genetic ablation of Ttyh1 blunted the basal nociceptive response and relieved the spontaneous nociception as well as hyperalgesia and allodynia in mice challenged by inflammatory irritants. Cumulatively, this study suggests and extends a newly-defined pivotal function for Ttyh1 in the initiation of pain transmission and sensitization caused by peripheral inflammation.

Ttyh1 Facilitates Pain *via* Enhancement of Nociceptor Excitability and Spinal Excitatory Synaptic Transmission

Another very intriguing finding of the present study is that we revealed the cellular basis for Ttyh1 in mediating pain transmission and sensitization. Compelling evidence indicates that peripheral pain-sensing neurons, called nociceptors, are a critical cellular origin of pain caused by inflammation or injury [47–52]. Abnormal hyperexcitability in nociceptors is a key driver for the generation of chronic pain states [28, 36, 48, 53, 54]. Taken together with the dense expression of Ttyh1 in nociceptors demonstrated in the present study, it is reasonable to speculate that Ttyh1 may facilitate pain and sensitization *via* enhancement of nociceptor excitability. Indeed, consistent with a previous report [55], small-diameter DRG neurons exhibited dramatic hyperexcitability upon peripheral inflammation in wild-type mice, as characterized by a heightened firing frequency and lowered rheobase. Deficiency of Ttyh1 did alleviate the magnitude of the hyperexcitability in nociceptors compared with Ttyh1$^{+/+}$ mice. Meanwhile, loss of Ttyh1 function also compromised the basal excitability of nociceptors. These results collectively led us to conclude that Ttyh1 plays a decisive role in determining nociceptor excitability.

The plasticity of synapses between nociceptor terminals and spinal neurons is considered as a cellular basis for the development and maintenance of pain hypersensitivity after peripheral inflammation or nerve injury [26, 27, 36, 56–58]. LTP can be triggered at spinal synapses between nociceptor terminals and spinal neurons projecting nociceptive information to the PAG by activated nociceptive afferents under conditioning stimulation at low

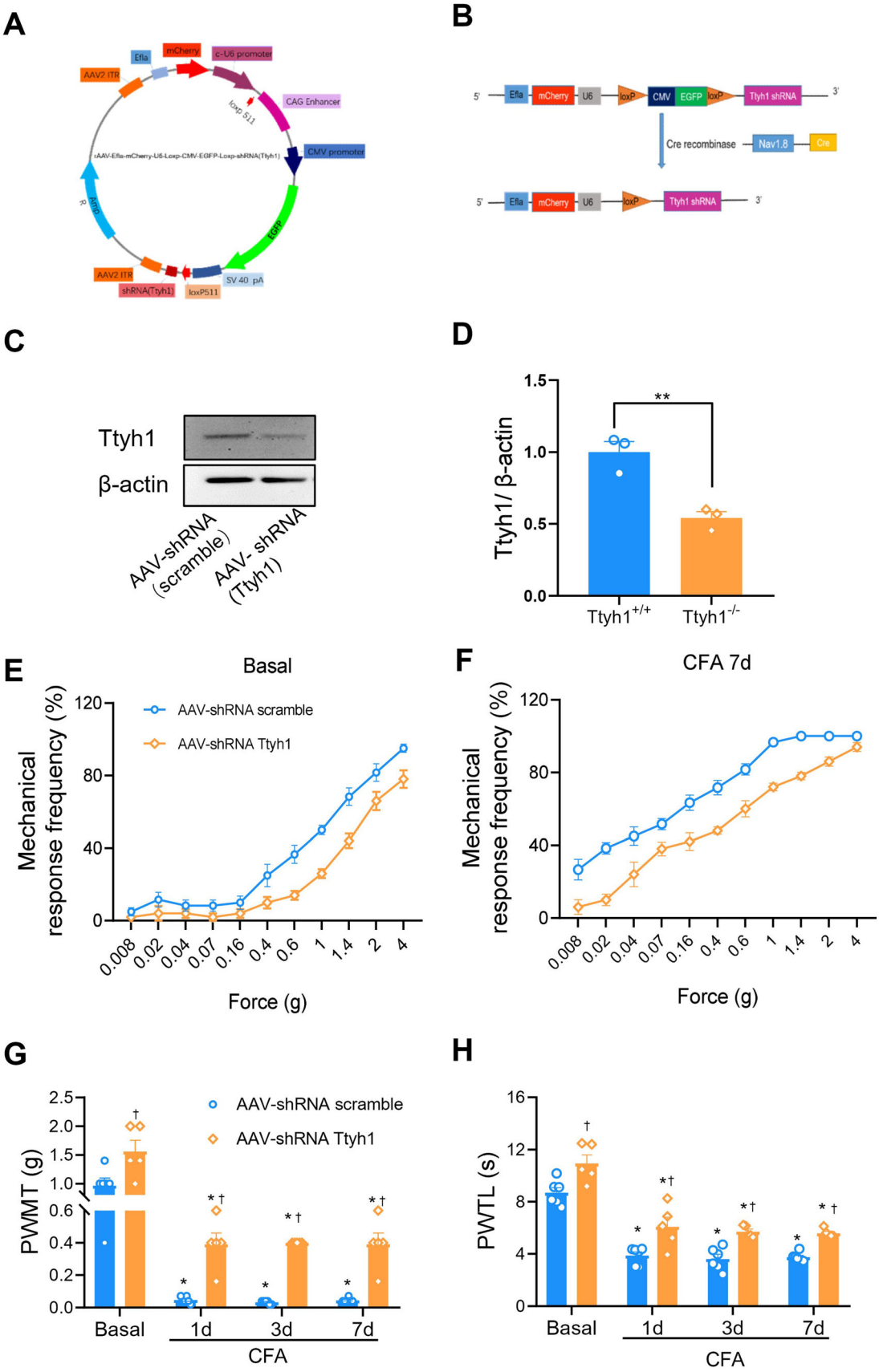
A
mCherry
c-U6 promoter
Efla
AAV2 ITR
CAG Enhancer
loxp 511
rAAV-Efla-mCherry-U6-Loxp-CMV-EGFP-Loxp-shRNA(Ttyh1)
CMV promoter
EGFP
AAV2 ITR
SV 40 pA
shRNA(Ttyh1)
loxP511
B
Efla
mCherry
U6
loxP
CMV
EGFP
loxP
Ttyh1 shRNA
Cre recombinase
Nav1.8
Cre
C
Ttyh1
β-actin
AAV-shRNA (scramble)
AAV- shRNA (Ttyh1)
D
Ttyh1/ β-actin
**
Ttyh1+/+
Ttyh1-/-
E
Basal
AAV-shRNA scramble
AAV-shRNA Ttyh1
Mechanical response frequency (%)
Force (g)
F
CFA 7d
Mechanical response frequency (%)
Force (g)
G
PWMT (g)
AAV-shRNA scramble
AAV-shRNA Ttyh1
Basal
1d
3d
7d
CFA
H
PWTL (s)
Basal
1d
3d
7d
CFA

◀**Fig. 7** Nociceptor-specific deficiency of Ttyh1 eliminates basal nociception and pain hypersensitivity caused by peripheral inflammation. **A, B** Schematics showing the strategy of nociceptor-specific knockdown of Ttyh1. **C, D** Typical examples (**C**) and quantitative summary (**D**) showing the efficiency of Ttyh1 knockdown in nociceptors. **E, F** Stimulus-response curves of specific knockdown of Ttyh1 in nociceptors reduces basal nociception and CFA-induced pain hypersensitivity. Stimulus-response curves to von Frey hairs at basal and after CFA injection (**E, F**), quantitative summary of PWMT (**G**) and PWTL (**H**) in SNS-Cre mice expressing shRNA Ttyh1 and scrambled shRNA in the L3/L4 dorsal root ganglia (DRGs). All data are presented as mean ± SEM. $^{*}P < 0.05$ *vs* basal, $^{\dagger}P < 0.05$ *vs* $Ttyh1^{+/+}$ mice.

frequencies relevant to pathological pain states or natural inflammatory irritation [25–27, 59]. This synaptic potentiation is assumed to require presynaptic mechanisms involving an increase in release probability from presynaptic nociceptor terminals [26, 27, 59]. Considering the crucial role of Ttyh1 in determining nociceptor excitability, we would expect that spinal synaptic transmission and potentiation may be subsequently regulated. In the present study, our patch-clamp recordings of C-eEPSCs in spinal-PAG projection neurons revealed that synaptic potentiation induced by either conditioning stimulation or natural CFA inflammation was greatly relieved by silencing Ttyh1. Spinal LTP evoked by a conditioning stimulus was even converted to LTD in $Ttyh1^{-/-}$ mice. Combined PPR and mEPSC analyses suggest a presynaptic origin of Ttyh1 function involving an increase of transmitter release probability. In addition, Ttyh1 also had a significant effect on basal synaptic transmission. This presynaptic regulation was strongly supported by our FISH data showing dense expression of Ttyh1 in CGRP-expressing peptidergic and IB4-binding non-peptidergic terminals in the SDH. Consistent with our results, Ttyh1 has also been found along axons and in the presynaptic active zone in supraspinal regions such as the hippocampus [17, 60].

Exactly how Ttyh1 accomplishes this is unknown so far. Several studies using transfected cells have indicated a putative function for the tty family proteins as maxi-Cl^- ion channels, with Ttyh1 encoding volume-regulated Cl^- channels that are activated by cell swelling, and Ttyh2 and Ttyh3 encoding Ca^{2+}-activated Cl^- channels [12–14, 16, 61]. There is evidence that cell volume is challenged not only under physiological conditions, such as nutrient accumulation, epithelial absorption, neurohormone and autocrine stimulation, as well as chemokine stimulation, but also under pathophysiological conditions such as hypoxia, ischemia, hyponatremia, and intracellular acidosis [62]. Peripheral inflammation often causes the release of various inflammatory mediators from inflamed tissues, including prostaglandins, histamine, bradykinin, chemokines, and protons [63, 64], which may lead to changes in cell volume such as cell swelling and in turn activates Ttyh1-encoded volume-regulated Cl^- channels in nociceptors. Previous studies have reported a higher tonic concentration of Cl^- ($[Cl^-]$) in peripheral sensory neurons and even further intracellular Cl^- ($[Cl^-]_i$) accumulation in response to inflammation, leading to equilibrium potentials of Cl^- values in the range of – 50 to – 10 mV, which is much higher than the RMP [65, 66]. Thus, activation of Ttyh1-encoded Cl^- channels is able to cause Cl^- efflux and produce a depolarizing inward current, resulting in nociceptor sensitization. This assumption remains to be further clarified in a future studies. Besides the presumed volume-regulated Cl^- channels from transfected cells, alternative *in vivo* evidence indicates that Ttyh1 is a Ca^{2+}-binding protein localized in the endoplasmic reticulum that is necessary for early embryogenesis by maintaining Ca^{2+} homeostasis [23]. Whether Ttyh1 acts as a Ca^{2+}-binding protein in nociceptive sensory neurons needs further investigation.

Targeting Peripheral Ttyh1 May Represent a Novel Therapeutic Intervention for Analgesia with Minimal Side-Effects

Abundant experimental and clinical evidence has shown that ongoing nociceptive primary afferent inputs are the key drivers for the development and maintenance of chronic pain [28, 36, 47–52, 54]. Once the afferent input from the affected area is removed, pain hypersensitivity and the associated aversive disorders caused by inflammation or injury are abolished [48, 50]. Lidocaine administration at the injured site has been applied to and gained prominent pain relief in a variety of chronic pain conditions [48–50, 67, 68]. However, since Na^+ channels are expressed in all neurons and fibers, lidocaine application may block normal sensory and motor function along with pain. To reduce this side-effect, in the present study, we identified a new target, Ttyh1 especially in nociceptors, in pain transmission and sensitization. Selective ablation of Ttyh1 in nociceptors had an antinociceptive effect comparable to global $Ttyh1^{-/-}$ mice. Loss of Ttyh1 strongly depressed nociceptor hyperexcitability and spinal synaptic potentiation *via* presynaptic mechanisms under inflammatory pain states. Since nociceptors are located in the periphery, pharmacological inhibitors of Ttyh1 need not enter the central nervous system and can hence minimize the central side-effects without sacrificing analgesic efficacy.

In summary, this study sheds new light on the functional role of Ttyh1 in the pain transmission and sensitization caused by peripheral inflammation. Further mechanistic analysis revealed that nociceptor-localized Ttyh1 is well placed to orchestrate nociceptor hyperexcitability and spinal synaptic potentiation *via* presynaptic mechanisms,

thereby providing a basis for opening up a novel therapeutic target to prevent inflammatory pain chronicity with minimal side-effects.

Acknowledgements This work was supported by the National Natural Science Foundation of China (31671088 and 31730041) and the Natural Science Foundation of Shaanxi Province, China (2017ZDJC-01).

Conflict of interest The authors declare that they have no conflict of interests.

References

1. Woolf CJ. What is this thing called pain? J Clin Invest 2010, 120: 3742–3744.
2. Ji RR. Recent progress in understanding the mechanisms of pain and itch: the second special issue. Neurosci Bull 2018, 34: 1–3.
3. Finnerup NB, Jensen TS. Mechanisms of disease: mechanism-based classification of neuropathic pain-a critical analysis. Nat Clin Pract Neurol 2006, 2: 107–115.
4. Finnerup NB, Sindrup SH, Jensen TS. Chronic neuropathic pain: mechanisms, drug targets and measurement. Fundam Clin Pharmacol 2007, 21: 129–136.
5. Gereau RWt, Sluka KA, Maixner W, Savage SR, Price TJ, Murinson BB, *et al*. A pain research agenda for the 21st century. J Pain 2014, 15: 1203–1214.
6. Weisberg DF, Becker WC, Fiellin DA, Stannard C. Prescription opioid misuse in the United States and the United Kingdom: cautionary lessons. Int J Drug Policy 2014, 25: 1124–1130.
7. Stoicea N, Costa A, Periel L, Uribe A, Weaver T, Bergese SD. Current perspectives on the opioid crisis in the US healthcare system: a comprehensive literature review. Medicine (Baltimore) 2019, 98: e15425.
8. Grosser T, Woolf CJ, FitzGerald GA. Time for nonaddictive relief of pain. Science 2017, 355: 1026–1027.
9. Dowell D, Haegerich TM, Chou R. CDC guideline for prescribing opioids for chronic pain - United States, 2016. MMWR Recomm Rep 2016, 65: 1–49.
10. Moore RA, Derry S, Simon LS, Emery P. Nonsteroidal anti-inflammatory drugs, gastroprotection, and benefit-risk. Pain Pract 2014, 14: 378–395.
11. Campbell HD, Schimansky T, Claudianos C, Ozsarac N, Kasprzak AB, Cotsell JN, *et al*. The *Drosophila melanogaster* flightless-I gene involved in gastrulation and muscle degeneration encodes gelsolin-like and leucine-rich repeat domains and is conserved in *Caenorhabditis elegans* and humans. Proc Natl Acad Sci U S A 1993, 90: 11386–11390.
12. Campbell HD, Kamei M, Claudianos C, Woollatt E, Sutherland GR, Suzuki Y, et al. Human and mouse homologues of the *Drosophila melanogaster tweety* (*tty*) gene: a novel gene family encoding predicted transmembrane proteins. Genomics 2000, 68: 89–92.
13. Rae FK, Hooper JD, Eyre HJ, Sutherland GR, Nicol DL, Clements JA. *TTYH2*, a human homologue of the *Drosophila melanogaster* gene *tweety*, is located on 17q24 and upregulated in renal cell carcinoma. Genomics 2001, 77: 200–207.
14. Suzuki M, Mizuno A. A novel human Cl^- channel family related to *Drosophila flightless* locus. J Biol Chem 2004, 279: 22461–22468.
15. Suzuki M. The *Drosophila tweety* family: molecular candidates for large-conductance Ca^{2+}-activated Cl^- channels. Exp Physiol 2006, 91: 141–147.
16. Han YE, Kwon J, Won J, An H, Jang MW, Woo J, *et al*. Tweety-homolog (*Ttyh*) family encodes the pore-forming subunits of the swelling-dependent volume-regulated anion channel ($VRAC_{swell}$) in the brain. Exp Neurobiol 2019, 28: 183–215.
17. Matthews CA, Shaw JE, Hooper JA, Young IG, Crouch MF, Campbell HD. Expression and evolution of the mammalian brain gene *Ttyh1*. J Neurochem 2007, 100: 693–707.
18. Stefaniuk M, Lukasiuk K. Cloning of expressed sequence tags (ESTs) representing putative epileptogenesis-related genes and the localization of their expression in the normal brain. Neurosci Lett 2010, 482: 230–234.
19. Stefaniuk M, Swiech L, Dzwonek J, Lukasiuk K. Expression of Ttyh1, a member of the Tweety family in neurons *in vitro* and *in vivo* and its potential role in brain pathology. J Neurochem 2010, 115: 1183–1194.
20. Kleinman CL, Gerges N, Papillon-Cavanagh S, Sin-Chan P, Pramatarova A, Quang DA, *et al*. Fusion of *TTYH1* with the C19MC microRNA cluster drives expression of a brain-specific *DNMT3B* isoform in the embryonal brain tumor ETMR. Nat Genet 2014, 46: 39–44.
21. Wu HN, Cao XL, Fang Z, Zhang YF, Han WJ, Yue KY, *et al*. Deficiency of Ttyh1 downstream to Notch signaling results in precocious differentiation of neural stem cells. Biochem Biophys Res Commun 2019, 514: 842–847.
22. Halleran AD, Sehdev M, Rabe BA, Huyck RW, Williams CC, Saha MS. Characterization of tweety gene (*ttyh1-3*) expression in *Xenopus laevis* during embryonic development. Gene expr patterns 2015, 17: 38–44.
23. Kumada T, Yamanaka Y, Kitano A, Shibata M, Awaya T, Kato T, *et al*. Ttyh1, a Ca^{2+}-binding protein localized to the endoplasmic reticulum, is required for early embryonic development. Dev Dyn 2010, 239: 2233–2245.
24. Al-Jumaily M, Kozlenkov A, Mechaly I, Fichard A, Matha V, Scamps F, *et al*. Expression of three distinct families of calcium-activated chloride channel genes in the mouse dorsal root ganglion. Neurosci Bull 2007, 23: 293–299.
25. Ikeda H, Stark J, Fischer H, Wagner M, Drdla R, Jager T, *et al*. Synaptic amplifier of inflammatory pain in the spinal dorsal horn. Science 2006, 312: 1659–1662.
26. Luo C, Gangadharan V, Bali KK, Xie RG, Agarwal N, Kurejova M, *et al*. Presynaptically localized cyclic GMP-dependent protein kinase 1 is a key determinant of spinal synaptic potentiation and pain hypersensitivity. PLoS Biol 2012, 10: e1001283.
27. Luo C, Kuner T, Kuner R. Synaptic plasticity in pathological pain. Trends Neurosci 2014, 37: 343–355.
28. Woolf CJ, Ma Q. Nociceptors—Noxious stimulus detectors. Neuron 2007, 55: 353–364.
29. Sandkuhler J. Translating synaptic plasticity into sensation. Brain 2015, 138: 2463–2464.
30. Chen J, Luo C, Li H, Chen H. Primary hyperalgesia to mechanical and heat stimuli following subcutaneous bee venom injection into the plantar surface of hindpaw in the conscious rat: a comparative study with the formalin test. Pain 1999, 83: 67–76.
31. Guo B, Chen J, Chen Q, Ren K, Feng D, Mao H, *et al*. Anterior cingulate cortex dysfunction underlies social deficits in *Shank3* mutant mice. Nat Neurosci 2019, 22: 1223–1234.
32. Huang J, Chen J, Wang W, Wang W, Koshimizu Y, Wei YY, *et al*. Neurochemical properties of enkephalinergic neurons in lumbar spinal dorsal horn revealed by preproenkephalin-green fluorescent protein transgenic mice. J Neurochem 2010, 113: 1555–1564.
33. Wittmann G, Hrabovszky E, Lechan RM. Distinct glutamatergic and GABAergic subsets of hypothalamic pro-opiomelanocortin neurons revealed by in situ hybridization in male rats and mice. J Comp Neurol 2013, 521: 3287–3302.

34. Cao XL, Zhang X, Zhang YF, Zhang YZ, Song CG, Liu F, *et al*. Expression and purification of mouse Ttyh1 fragments as antigens to generate Ttyh1-specific monoclonal antibodies. Protein Expres Purif 2017, 130: 81–89.
35. Sun W, Miao B, Wang XC, Duan JH, Wang WT, Kuang F, *et al*. Reduced conduction failure of the main axon of polymodal nociceptive C-fibres contributes to painful diabetic neuropathy in rats. Brain 2012, 135: 359–375.
36. Sun W, Miao B, Wang XC, Duan JH, Ye X, Han WJ, *et al*. Gastrodin inhibits allodynia and hyperalgesia in painful diabetic neuropathy rats by decreasing excitability of nociceptive primary sensory neurons. PLoS One 2012, 7: e39647.
37. Xie RG, Gao YJ, Park CK, Lu N, Luo C, Wang WT, *et al*. Spinal CCL2 promotes central sensitization, long-term potentiation, and inflammatory pain via CCR2: further insights into molecular, synaptic, and cellular mechanisms. Neurosci Bull 2018, 34: 13–21.
38. Nakatsuka T, Ataka T, Kumamoto E, Tamaki T, Yoshimura M. Alteration in synaptic inputs through C-afferent fibers to substantia gelatinosa neurons of the rat spinal dorsal horn during postnatal development. Neuroscience 2000, 99: 549–556.
39. Luo C, Kumamoto E, Furue H, Chen J, Yoshimura M. Nociceptin inhibits excitatory but not inhibitory transmission to substantia gelatinosa neurones of adult rat spinal cord. Neuroscience 2002, 109: 349–358.
40. Nam BY, Kim DK, Park JT, Kang HY, Paeng J, Kim S, *et al*. Double transduction of a Cre/LoxP lentiviral vector: a simple method to generate kidney cell-specific knockdown mice. Am J Physiol Renal Physiol 2015, 309: F1060–1069.
41. Tjolsen A, Berge OG, Hunskaar S, Rosland JH, Hole K. The formalin test: an evaluation of the method. Pain 1992, 51: 5–17.
42. Schulz PE, Cook EP, Johnston D. Using paired-pulse facilitation to probe the mechanisms for long-term potentiation (LTP). J Physiol Paris 1995, 89: 3–9.
43. Han WJ, Zhao ZW, Du YK, Xiao MM, Xie RG, Luo C. Characteristics of short-term synaptic plasticity of spino-PAG projection neurons in the lamina I of spinal dorsal horn of mice (in chinese). Chinese Journal of Neuroanatomy 2017, 33: 111–116.
44. Agarwal N, Offermanns S, Kuner R. Conditional gene deletion in primary nociceptive neurons of trigeminal ganglia and dorsal root ganglia. Genesis 2004, 38: 122–129.
45. Wiernasz E, Kaliszewska A, Brutkowski W, Bednarczyk J, Gorniak M, Kaza B, *et al*. Ttyh1 protein is expressed in glia *in vitro* and shows elevated expression in activated astrocytes following status epilepticus. Neurochem Res 2014, 39: 2516–2526.
46. Kim J, Han D, Byun SH, Kwon M, Cho JY, Pleasure SJ, *et al*. Ttyh1 regulates embryonic neural stem cell properties by enhancing the Notch signaling pathway. EMBO Rep 2018, 19: e45472.
47. Campbell JN, Meyer RA. Mechanisms of neuropathic pain. Neuron 2006, 52: 77–92.
48. Haroutounian S, Nikolajsen L, Bendtsen TF, Finnerup NB, Kristensen AD, Hasselstrom JB, *et al*. Primary afferent input critical for maintaining spontaneous pain in peripheral neuropathy. Pain 2014, 155: 1272–1279.
49. Haroutounian S, Ford AL, Frey K, Nikolajsen L, Finnerup NB, Neiner A, *et al*. How central is central poststroke pain? The role of afferent input in poststroke neuropathic pain: a prospective, open-label pilot study. Pain 2018, 159: 1317–1324.
50. Vaso A, Adahan HM, Gjika A, Zahaj S, Zhurda T, Vyshka G, *et al*. Peripheral nervous system origin of phantom limb pain. Pain 2014, 155: 1384–1391.
51. Daou I, Beaudry H, Ase AR, Wieskopf JS, Ribeiro-da-Silva A, Mogil JS, *et al*. Optogenetic silencing of Nav1.8-positive afferents alleviates inflammatory and neuropathic pain. eNeuro 2016, 3: 1–12.
52. Cowie AM, Moehring F, O'Hara C, Stucky CL. Optogenetic inhibition of CGRPalpha sensory neurons reveals their distinct roles in neuropathic and incisional pain. J Neurosci 2018, 38: 5807–5825.
53. Nordin M, Nystrom B, Wallin U, Hagbarth KE. Ectopic sensory discharges and paresthesiae in patients with disorders of peripheral nerves, dorsal roots and dorsal columns. Pain 1984, 20: 231–245.
54. Devor M. Neuropathic pain: pathophysiological response of nerves to injury. In: Wall and Melzack's textbook of pain. 6th ed. London: Churchill Livingstone, 2013: 861–888.
55. Pitake S, Middleton LJ, Abdus-Saboor I, Mishra SK. Inflammation induced sensory nerve growth and pain hypersensitivity requires the N-type calcium channel Cav2.2. Front Neurosci 2019, 13: 1009.
56. Woolf CJ, Salter MW. Neuronal plasticity: increasing the gain in pain. Science 2000, 288: 1765–1769.
57. Basbaum AI, Bautista DM, Scherrer G, Julius D. Cellular and molecular mechanisms of pain. Cell 2009, 139: 267–284.
58. Sandkuhler J. Models and mechanisms of hyperalgesia and allodynia. Physiol Rev 2009, 89: 707–758.
59. Xiao MM, Zhang YQ, Wang WT, Han WJ, Lin Z, Xie RG, *et al*. Gastrodin protects against chronic inflammatory pain by inhibiting spinal synaptic potentiation. Sci Rep 2016, 6: 37251.
60. Morciano M, Beckhaus T, Karas M, Zimmermann H, Volknandt W. The proteome of the presynaptic active zone: from docked synaptic vesicles to adhesion molecules and maxi-channels. J Neurochem 2009, 108: 662–675.
61. Bae Y, Kim A, Cho CH, Kim D, Jung HG, Kim SS, *et al*. TTYH1 and TTYH2 serve as LRRC8A-independent volume-regulated anion channels in cancer cells. Cells 2019, 8: 562.
62. Lambert IH, Hoffmann EK, Pedersen SF. Cell volume regulation: physiology and pathophysiology. Acta Physiol (Oxf) 2008, 194: 255–282.
63. Millan MJ. The induction of pain: an integrative review. Prog Neurobiol 1999, 57: 1–164.
64. Meyer R, Ringkamp M, Campbell J, Raja S. Peripheral mechanisms of cutaneous nociception. In: Wall and Melzack's textbook of pain. 6th ed. London: Churchill Livingstone, 2013, 8–19.
65. Funk K, Woitecki A, Franjic-Wurtz C, Gensch T, Mohrlen F, Frings S. Modulation of chloride homeostasis by inflammatory mediators in dorsal root ganglion neurons. Mol Pain 2008, 4: 32.
66. Gilbert D, Franjic-Wurtz C, Funk K, Gensch T, Frings S, Mohrlen F. Differential maturation of chloride homeostasis in primary afferent neurons of the somatosensory system. Int J Dev Neurosci 2007, 25: 479–489.
67. Nair AS, Mantha SSP, Azharuddin M, Rayani BK. Lidocaine 5% patch in localized neuropathic pain. Indian J Palliat Care 2019, 25: 594–595.
68. Pickering G, Voute M, Macian N, Ganry H, Pereira B. Effectiveness and safety of 5% lidocaine-medicated plaster on localized neuropathic pain after knee surgery: a randomized, double-blind controlled trial. Pain 2019, 160: 1186–1195.